

# The earliest unequivocally modern humans in southern China

Wu Liu<sup>1\*</sup>, María Martín-Torres<sup>2,3,4\*</sup>, Yan-jun Cai<sup>5</sup>, Song Xing<sup>1</sup>, Hao-wen Tong<sup>1</sup>, Shu-wen Pei<sup>1</sup>, Mark Jan Sier<sup>4,6,7</sup>, Xiao-hong Wu<sup>8</sup>, R. Lawrence Edwards<sup>9</sup>, Hai Cheng<sup>10</sup>, Yi-yuan Li<sup>11</sup>, Xiong-xin Yang<sup>12</sup>, José María Bermúdez de Castro<sup>2,4</sup> & Xiu-jie Wu<sup>1\*</sup>

**The hominin record from southern Asia for the early Late Pleistocene epoch is scarce. Well-dated and well-preserved fossils older than ~45,000 years that can be unequivocally attributed to *Homo sapiens* are lacking<sup>1–4</sup>. Here we present evidence from the newly excavated Fuyan Cave in Daoxian (southern China). This site has provided 47 human teeth dated to more than 80,000 years old, and with an inferred maximum age of 120,000 years. The morphological and metric assessment of this sample supports its unequivocal assignment to *H. sapiens*. The Daoxian sample is more derived than any other anatomically modern humans, resembling middle-to-late Late Pleistocene specimens and even contemporary humans. Our study shows that fully modern morphologies were present in southern China 30,000–70,000 years earlier than in the Levant and Europe<sup>5–7</sup>. Our data fill a chronological and geographical gap that is relevant for understanding when *H. sapiens* first appeared in southern Asia. The Daoxian teeth also support the hypothesis that during the same period, southern China was inhabited by more derived populations than central and northern China. This evidence is important for the study of dispersal routes of modern humans. Finally, our results are relevant to exploring the reasons for the relatively late entry of *H. sapiens* into Europe. Some studies have investigated how the competition with *H. sapiens* may have caused Neanderthals' extinction (see ref. 8 and references therein). Notably, although fully modern humans were already present in southern China at least as early as ~80,000 years ago, there is no evidence that they entered Europe before ~45,000 years ago. This could indicate that *H. neanderthalensis* was indeed an additional ecological barrier for modern humans, who could only enter Europe when the demise of Neanderthals had already started.**

The Fuyan Cave (25° 39' 02.7" N, 111° 28' 49.2" E; 232 m above sea level) is located in Tangbei Village, Daoxian County, Hunan Province, southern China (Fig. 1). It is part of a large multi-genesis pipeline-type karst system that contains several connected and stacked caves (Supplementary Information A), and covers an area of more than 3,000 m<sup>2</sup>. The investigation and excavations were conducted at three regions in the cave, regions I, II and III (Extended Data Fig. 1). From 2011 to 2013, systematic excavations yielded 47 human teeth and an abundant fossil mammalian assemblage (Fig. 2 and Extended Data Figs 2 and 3).

Four clear stratigraphic layers were consistently identified in the whole excavated regions (regions I, II and III), with a total thickness of more than 250 cm (Fig. 1). All the hominin and mammalian fossils were found in layer 2 of region I (mammals) and region II (mammals and humans), although three human teeth (DX1, DX2 and DX6) and a

small amount of mammalian fossils were found out of context as surface findings during the first year of excavation. The stratigraphic sequence of region II, from top to bottom, is described as follows: (1) layer 1: continuous brown-grey and brown-yellow flowstone/calcite-cemented deposit with a maximum thickness of 20 cm; (2) layer 2: brown-yellow and grey fine sandy clay of 20–50 cm in thickness that contains a large amount of mammalian fossils and the hominin teeth; (3) layer 3: brown and grey sandy gravel of 80–100 cm in thickness; and (4) layer 4: grey-yellow and brown-yellow silt and clay with calcareous breccia imbedded. This layer is more than 100 cm in thickness as the bottom has not been reached yet.

At present, no stone tools have been found. The hominin and most of the faunal elements consist exclusively of teeth, and many of them present root alterations mostly due to the effects of calcium dissolution and some rodent gnawing (Supplementary Information B). The mammalian fossil assemblage from the Daoxian site is typical of Late Pleistocene in southern China, and is composed of 38 species including 5 extinct large mammals such as *Ailuropoda baconi*, *Crocota ultima*, *Stegodon orientalis*, *Megatapirus augustus* and *Sus* sp. (Extended Data Table 1 and Supplementary Information C). The radiocarbon age older than 43,000 calibrated years BP (43 kyr cal BP) obtained for one of the faunal remains (see Supplementary Information D) supports its pre-late Late Pleistocene age.

During the excavations, we collected nine samples of speleothem fragments from layers 2 to 3 (FYS-1 to FYS-9) at regions I and II, and two subsamples (FYS-S1 to FYS-S2) from a small stalagmite that grew on the top of layer 1 (Fig. 1, Extended Data Fig. 1 and Supplementary Information E). These samples were carefully preprocessed to single out the clean portion for <sup>230</sup>Th dating, and then analysed at the Isotope Lab of University of Minnesota using the multicollector-inductively coupled plasma-mass spectrometry (MC-ICP-MS) dating technique<sup>9</sup>. Eight speleothem fragments from layer 2 yielded Middle to Late Pleistocene ages ranging from ~556 kyr BP to 120.7 kyr BP, and one sample collected from layer 3 (FYS-9) provided an age older than 600 kyr BP and thus, beyond the limit of the <sup>230</sup>Th dating method (Table 1). The two subsamples from the small stalagmite give an age of 80.1 ± 1.2 kyr BP and 79.5 ± 2.8 kyr BP (mean ± 2 s.d.), respectively.

The calcitic floor (layer 1) is encrusted on layer 2, and is continuous across the excavated regions, preventing younger material from being introduced into the underlying deposits (see Supplementary Information, Cave Tour). The abundant and extensive distribution of the fauna and human teeth across the cave makes re-deposition of layer 2 highly unlikely. In addition, palaeomagnetic and rock-magnetic analysis of a sample layer 1 at region IIA confirms that

<sup>1</sup>Key Laboratory of Vertebrate Evolution and Human Origins of Chinese Academy of Sciences, Institute of Vertebrate Paleontology and Paleoanthropology, Chinese Academy of Sciences, Beijing 100044, China. <sup>2</sup>UCL Anthropology, 14 Taviston Street, London WC1H 0BW, UK. <sup>3</sup>Departamento de Ciencias Históricas y Geografía, University of Burgos, Hospital del Rey, s/n. 09001 Burgos, Spain. <sup>4</sup>Centro Nacional de Investigación sobre la Evolución Humana (CENIEH), Paseo Sierra de Atapuerca 3, 09002 Burgos, Spain. <sup>5</sup>State Key Laboratory of Loess and Quaternary Geology, Institute of Earth Environment, Chinese Academy of Sciences, Xian 710075, China. <sup>6</sup>Paleomagnetic Laboratory 'Fort Hoofddijk', Department of Earth Sciences, Faculty of Geosciences, Utrecht University, Budapestlaan 17, 3584 CD Utrecht, The Netherlands. <sup>7</sup>Faculty of Archaeology, Leiden University, PO Box 9515, 2300 RA Leiden, The Netherlands. <sup>8</sup>School of Archaeology and Museology, Peking University, Beijing 100871, China. <sup>9</sup>Department of Geology and Geophysics, University of Minnesota, Minneapolis, Minnesota 55455, USA. <sup>10</sup>Institute of Global Environmental Change, Xi'an Jiaotong University, Xi'an 710049, China. <sup>11</sup>Institute of Cultural Relics and Archaeology, Hunan Province, Changsha 410008, China. <sup>12</sup>Cultural Relics Administration of Daoxian County, Daoxian 425300, China.

\*These authors contributed equally to this work.

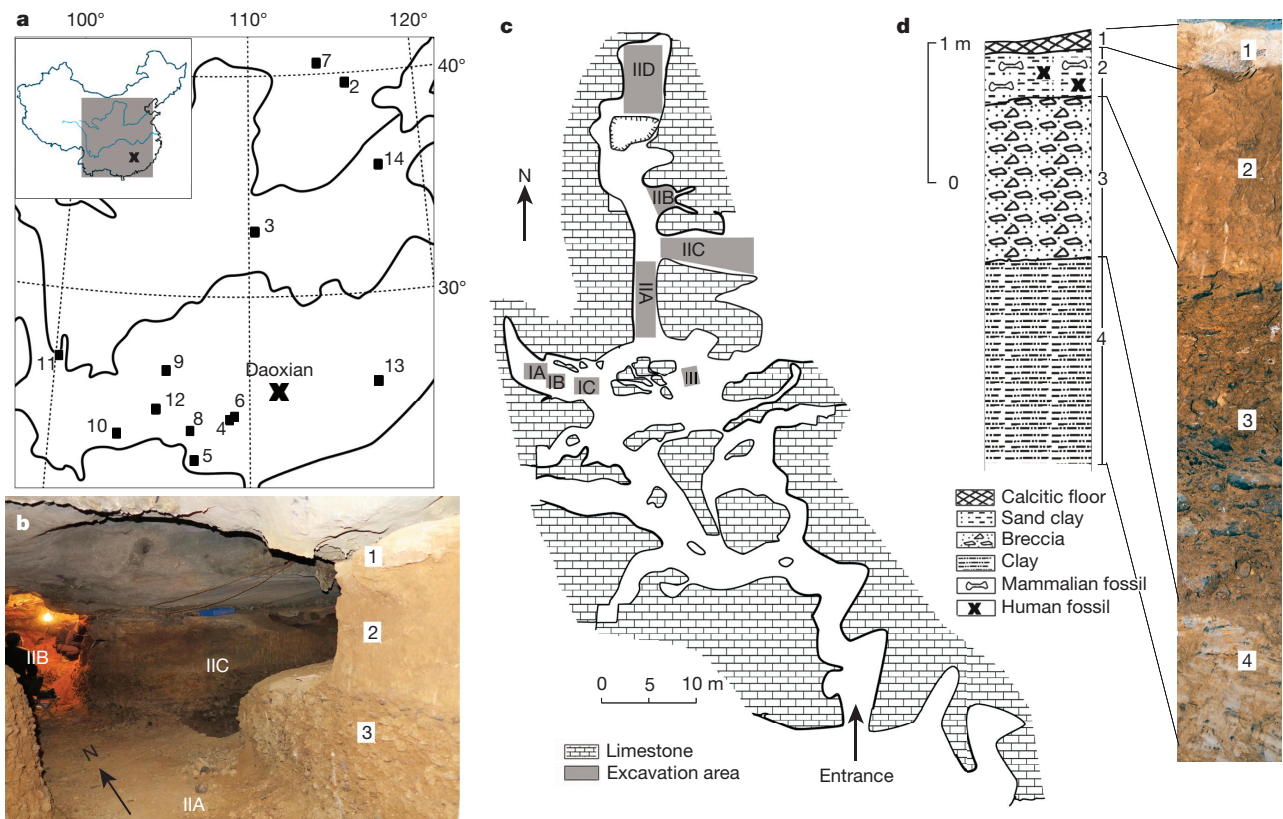


**Figure 1 | Geographical location and stratigraphy of the Daoxian site.** **a**, Location of the Daoxian site. Late Middle Pleistocene and Late Pleistocene localities with human remains that have been included in the morphological and/or metric comparison with Daoxian are also marked on the map. 2: Tianyuan Cave; 3: Huanglong Cave; 4: Liujiang; 5: Zhiren Cave; 6: Tubo; 7: Xujiayao; 8: Luna; 9: Chuandong; 10: Malu Cave; 11: Lijiang; 12: Longlin; 13: Huli Cave; and 14: Xintai. The map is adapted from the original Chinese map

from National Administration of Surveying, Mapping and Geoinformation of China (<http://219.238.166.215/mcp/index.asp>). **b**, General view of the interior of the cave and the spatial relationship of regions IIA, IIB and IIC, with some of the layers marked. **c**, Plan view of the excavation area. **d**, Detail of the stratigraphic layers of region II of the Daoxian site. All human fossils come from layer 2.

the flowstone that caps the fossil-bearing layer 2 remains *in situ* (Supplementary Information F and Extended Data Fig. 4). Therefore, the dated stalagmite was formed after the fossils were buried and it provides a minimum age constraint (~80 kyr) for the fossils below. Because the associated fauna is typical of the Late Pleistocene, we conservatively assume that fossils are not older than ~120 kyr, and

the presence of hominins at Daoxian can be bracketed between 80 kyr and 120 kyr.

Daoxian teeth were compared to large dental samples of Late Pleistocene hominin fossils from Europe, Africa and Asia (Extended Data Tables 2 and 3 and Supplementary Information G and H). The Daoxian teeth are small and they consistently fall within *H. sapiens*

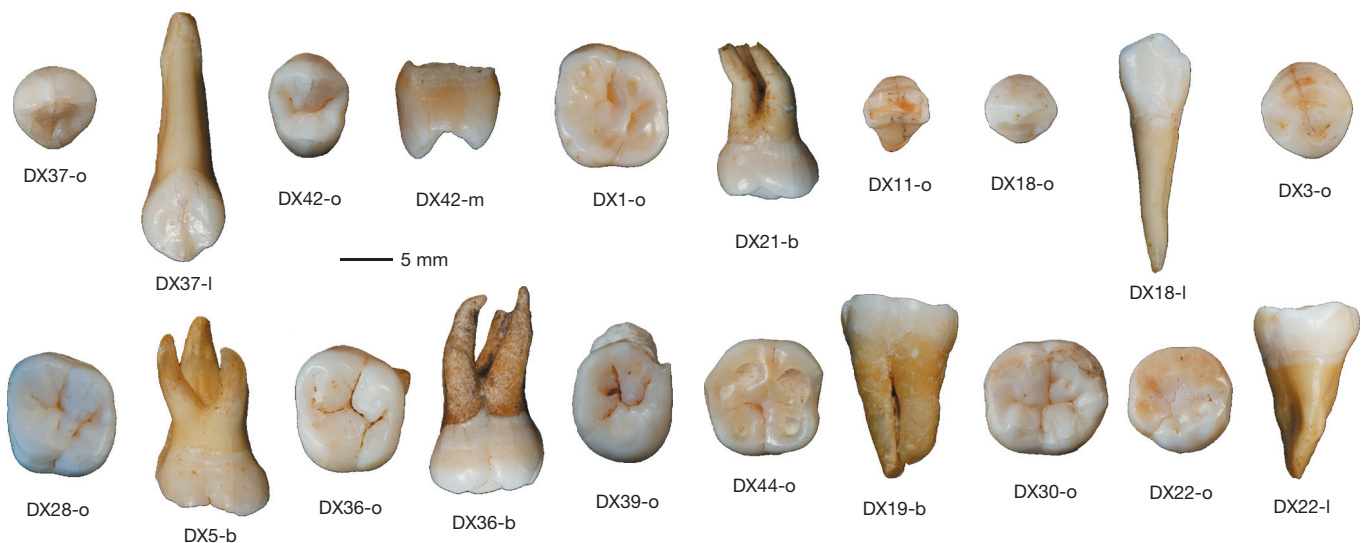


**Figure 2 | Daoxian human teeth (selection).** See Extended Data Table 2 for detailed information about each tooth. b, buccal; d, distal; l, lingual, m, mesial; o, occlusal. Credits: S.X. and X.-J.W.

**Table 1 | The <sup>230</sup>Th ages of the Daoxian site**

Sample ID	Region/layer	<sup>238</sup> U (ppb)	<sup>232</sup> Th (ppt)	<sup>230</sup> Th/ <sup>232</sup> Th (atomic ×10 <sup>-6</sup> )	δ <sup>234</sup> U* (measured)	<sup>230</sup> Th/ <sup>238</sup> U (activity)	<sup>230</sup> Th age (kyr BP) (uncorrected)	δ <sup>234</sup> U <sub>initial</sub> † (corrected)	<sup>230</sup> Th age (kyr BP)‡ (corrected)
FYS-S1	IID/layer 1	133.3 ± 0.3	9,117 ± 183	176.5 ± 3.6	353.1 ± 4.5	0.7326 ± 0.0033	81.5 ± 0.7	443 ± 6	80.1 ± 1.2
FYS-S2	IID/layer 1	285.9 ± 0.4	55,026 ± 1,102	64.0 ± 1.3	356.2 ± 3.2	0.7467 ± 0.0026	83.4 ± 0.5	446 ± 5	79.5 ± 2.8
FYS-1	IIA/layer 2	428.2 ± 0.7	98,699 ± 1,976	59.4 ± 1.2	54.3 ± 2.1	0.8302 ± 0.0017	164.7 ± 1.2	85 ± 3	158.3 ± 4.6
FYS-2	IIA/layer 2	10,747.9 ± 69.1	27,564 ± 552	7,463.3 ± 149.9	633.0 ± 4.2	1.1609 ± 0.0077	121.0 ± 1.5	891 ± 7	121.0 ± 1.5
FYS-3	IC/layer 2	126.0 ± 0.2	8,675 ± 174	263.5 ± 5.3	75.6 ± 2.5	1.1000 ± 0.0027	558.3 ± 62.8	364 ± 67	556.8 ± 61.9
FYS-4	IB/layer 2	1,608.5 ± 5.5	889 ± 18	29,237 ± 588	401.0 ± 3.5	0.9800 ± 0.0035	120.7 ± 0.9	564 ± 5	120.7 ± 0.9
FYS-5	IB/layer 2	260.0 ± 0.4	41,356 ± 828	122.7 ± 2.5	173.3 ± 2.7	1.1837 ± 0.0026	351.5 ± 8.1	463 ± 13	348.3 ± 8.2
FYS-6	IA/layer 2	120.6 ± 0.2	81,358 ± 1,629	22.6 ± 0.5	171.4 ± 2.7	0.9236 ± 0.0027	158.5 ± 1.4	256 ± 10	141.8 ± 12.1
FYS-7	IID/layer 2	87.4 ± 0.1	12,302 ± 246	120.3 ± 2.5	187.8 ± 5.1	1.0276 ± 0.0055	196.1 ± 3.8	324 ± 10	192.9 ± 4.3
FYS-8	IID/layer 2	78.4 ± 0.2	20,571 ± 413	55.2 ± 1.1	157.4 ± 7.7	0.8786 ± 0.0044	147.1 ± 2.7	234 ± 12	140.7 ± 5.2
FYS-9	IIC/layer 3	267.6 ± 0.4	20,907 ± 419	10,618.9 ± 226.1	147.6 ± 3.2	2.5165 ± 0.3707	>600	-	-

\*δ<sup>234</sup>U = ((<sup>234</sup>U/<sup>238</sup>U)<sub>activity</sub> - 1) × 1,000.

†δ<sup>234</sup>U<sub>initial</sub> was calculated based on <sup>230</sup>Th age (T), that is, δ<sup>234</sup>U<sub>initial</sub> = δ<sup>234</sup>U<sub>measured</sub> × exp(λ<sub>234</sub> × T).

‡Corrected <sup>230</sup>Th ages assume the initial <sup>230</sup>Th/<sup>232</sup>Th atomic ratio of 4.4 ± 2.2 × 10<sup>-6</sup>. Those are the values for a material at secular equilibrium, with the bulk earth <sup>230</sup>Th/<sup>238</sup>U value of 3.8. The errors are arbitrarily assumed to be 50%.

BP stands for 'before present', in which 'present' is defined as the year 1950 AD. Values are mean ± 2 s.d.

variability (Fig. 3 and Extended Data Fig. 5). They are generally smaller than other Late Pleistocene specimens from Africa and Asia, and closer to European Late Pleistocene samples and contemporary modern humans. Both the crown and the root of Daoxian teeth show typical morphologies for *H. sapiens* (Fig. 2 and Extended Data Fig. 6), with simplified occlusal and labial/buccal surfaces and short and slender roots. The presence of moderate basal bulging as well as longitudinal grooves in the buccal surface of canines, premolars and molars from other Late Pleistocene samples such as Xujiayao, Huanglong Cave, Qafzeh or Dolni Vestonice make Daoxian teeth morphologically closer to middle-to-late Late Pleistocene and even contemporary human samples (Extended Data Fig. 6). Canine and molar roots are gracile and barely divergent, differing from the stout and robust root systems of Tubo or Xujiayao localities<sup>10</sup> where radicals do not narrow towards the tip (Extended Data Fig. 6). Indeed, the convergent apices of the molar buccal roots appear as a typical feature in contemporary *H. sapiens*. M<sup>1</sup> molars are also typical of *H. sapiens* and unlike the rhomboidal contour displayed by *H. neanderthalensis*<sup>11</sup> or the buccolingually elongated shape of Asian *H. erectus*<sup>12-14</sup>. The relative cusp and occlusal polygon areas of the Daoxian M<sup>1</sup> molars follow the *H. sapiens*

pattern and they only differ by 0.6% to 1.1% from modern Chinese populations (Extended Data Table 4). Interestingly, Qafzeh M<sup>1</sup>s are comparatively less derived than Daoxian, showing a departure from the typical *H. sapiens* pattern of cusp proportions and angles that were previously noticed<sup>11</sup>. The occlusal morphology of Daoxian M<sup>2</sup> and M<sup>3</sup>s is also simple, and both the metacone and the hypocone are strongly reduced as it is typical of *H. sapiens*. The lack of labial convexity, shovel shape and tuberculum dentale, as well as the gracile root of the Daoxian incisor I<sub>2</sub> resemble that of contemporary and Late Pleistocene *H. sapiens* and differs from Neanderthals. However, Dolni Vestonice specimens display higher labial convexity, and Qafzeh and Huanglong Cave I<sub>2</sub>s present a more prominent basal eminence, making Daoxian I<sub>2</sub> closer to contemporary humans rather than other Late Pleistocene samples. The two Daoxian P<sub>3</sub> premolars show a slightly asymmetric oval contour due to the disto-lingual projection of a small platform-like talonid without accessory cusps. Overall, the crown morphology together with the expression of a slender single root of Daoxian P<sub>3</sub>s is closer to *H. sapiens* and differs from the typical Neanderthal conformation, with compressed and centred occlusal polygon and lingually displaced metaconid<sup>15</sup>. Lower molars lack the typically

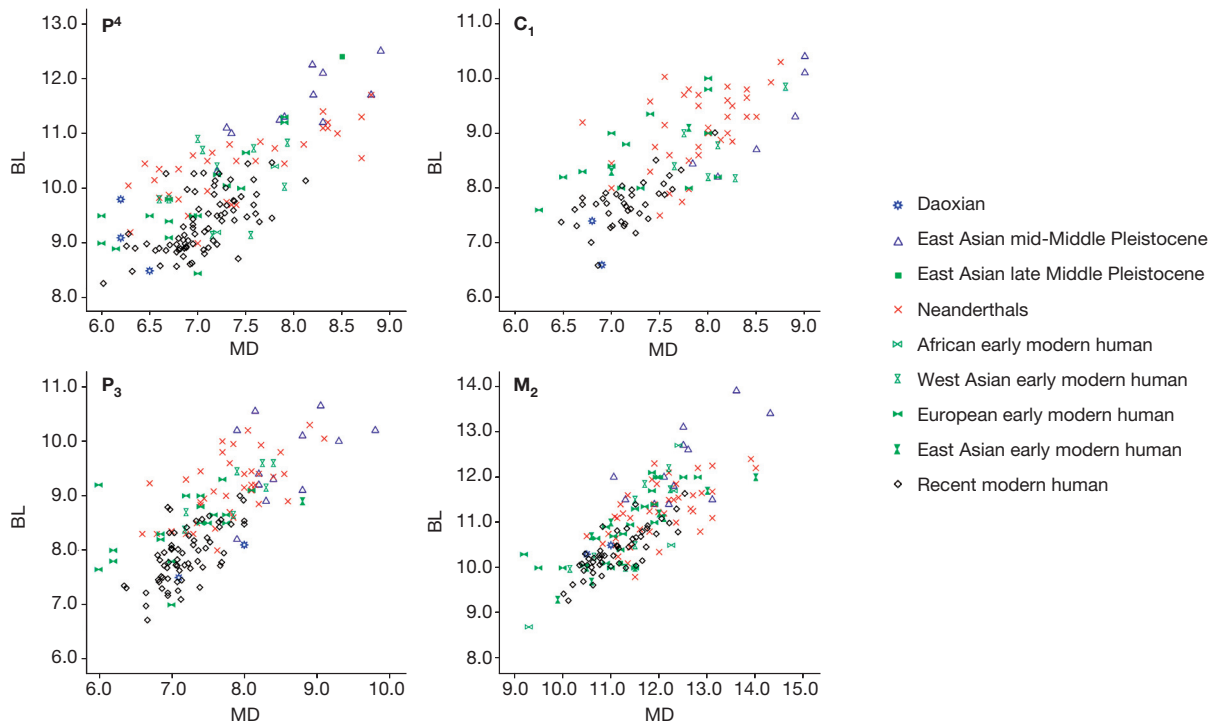


**Figure 3 | Metric comparison of Daoxian teeth.** Bivariate plots of the mesiodistal (MD) and buccolingual (BL) dimensions of the Daoxian upper fourth premolar (P<sup>4</sup>), lower canine (C<sub>1</sub>), lower third premolar (P<sub>3</sub>) and lower second molar (M<sub>2</sub>).

Neanderthal combination of a pit-like anterior fovea with a continuous mid-trigonal crest<sup>16,17</sup>. This, together with the reduction of the hypoconulid and the expression of an X-pattern in all the M<sub>2</sub> and M<sub>3</sub> where this feature could be recorded make Daoxian lower molars morphologically closer to anatomically and contemporary modern humans<sup>18</sup>. In addition, no signs of taurodontism are present. Finally, the occlusal morphology of the two upper second deciduous molars (dm<sup>2</sup>s) from Daoxian is simple, and the occlusal outline relatively squared and unlike the typical skewed contour of Neanderthals. Roots are thin and diverge as is typical in deciduous teeth, and similar to the patterns usually found in fossil and contemporary *H. sapiens*. Thus, the morphological and metric comparison of the Daoxian dental sample allows its unequivocal attribution to *H. sapiens*, and they present particular resemblances to late Late Pleistocene samples and contemporary modern humans.

At present, the earliest unambiguous evidence of *H. sapiens* fossils eastward of the Arabian Peninsula comes from Tianyuan Cave, in northern China<sup>19</sup>, Niah Cave in Borneo<sup>4</sup> and Lake Mungo in Australia<sup>20</sup> dated to ~40,000–50,000 years. The retention of primitive features in Qafzeh and Skhul has been interpreted by many as evidence of a 'failed' dispersal<sup>21,22</sup>, and several studies have recently suggested that an earlier and southern route may have been indeed more favourable for hominin expansion<sup>2,23–25</sup>. However, these and other related hypotheses were lacking the support of clear evidence of modern human occupation outside Africa (excluding the Levant) during the early Late Pleistocene. The fragmentary nature and/or the mosaic of modern and archaic features of remains such as those from the Zhiren Cave have prevented a unanimous acceptance of its taxonomic status<sup>1,26</sup>. This, together with the contested chronological-stratigraphic frame of some of the Asian hominin findings (see ref. 2 for a review), make the Daoxian teeth the earliest and soundest evidence of definitely modern humans in southern China at least 80 kyr ago. The Daoxian evidence may finally change the scepticism that most hypotheses considering the presence of *H. sapiens* in the early Late Pleistocene in China have been subjected to.

While the Daoxian findings would support the presence of fully modern populations in southern China during the early Late Pleistocene, the Xujiayao<sup>10</sup> and Denisova evidence<sup>27</sup> points to considerably more primitive hominins in the northern latitudes. Similarly, the dental morphology of the late Middle Pleistocene hominin from Panxian Dadong in southern China already exhibits some derived features<sup>28</sup> that are absent in other roughly contemporaneous Asian populations of higher latitudes, such as those from Zhoukoudian, Hexian or Chaoxian<sup>10</sup>. This evidence could support different origins and/or dispersal routes for modern humans across Asia<sup>23,24</sup>.

Finally, while fully modern humans succeeded to disperse throughout Asia during the early Late Pleistocene, they failed to do so in Europe until 35,000–75,000 years later. Thus, we should not rule out the possibility that *H. neanderthalensis* was for a long time an additional barrier for modern humans' expansion, who could only settle in Europe when Neanderthal populations started to fade.

**Online Content** Methods, along with any additional Extended Data display items and Source Data, are available in the online version of the paper; references unique to these sections appear only in the online paper.

Received 9 May; accepted 9 September 2015.

Published online 14 October 2015.

- Dennell, R. Early *Homo sapiens* in China. *Nature* **468**, 512–513 (2010).
- Dennell, R. in *Southern Asia, Australia and the Search for Human Origins* (eds Dennell, R. & Porr, M.) 33–50 (Cambridge Univ. Press, 2014).
- Storm, P. et al. U-series and radiocarbon analyses of human and faunal remains from Wajak, Indonesia. *J. Hum. Evol.* **64**, 356–365 (2013).
- Barker, G. et al. The 'human revolution' in lowland tropical Southeast Asia: the antiquity and behavior of anatomically modern humans at Niah Cave (Sarawak, Borneo). *J. Hum. Evol.* **52**, 243–261 (2007).
- Hershkovitz, I. et al. Levantine cranium from Manot Cave (Israel) foreshadows the first European modern humans. *Nature* **520**, 216–219 (2015).

- Grine, F. E. et al. Late Pleistocene human skull from Hofmeyr, South Africa, and modern human origins. *Science* **315**, 226–229 (2007).
- Benazzi, S. et al. The makers of the Protoaurignacian and implications for Neanderthal extinction. *Science* **348**, 793–796 (2015).
- Villa, P. & Roebroeks, W. Neanderthal demise: an archaeological analysis of the modern human superiority complex. *PLoS ONE* **9**, e96424 (2014).
- Cheng, H. et al. Improvements in <sup>230</sup>Th dating, <sup>230</sup>Th and <sup>234</sup>U half-life values, and U–Th isotopic measurements by multi-collector inductively coupled plasma mass spectrometry. *Earth Planet. Sci. Lett.* **371–372**, 82–91 (2013).
- Xing, S., Martín-Torres, M., Bermúdez de Castro, J. M., Wu, X. & Liu, W. Hominin teeth from the early Late Pleistocene site of Xujiayao, Northern China. *Am. J. Phys. Anthropol.* **156**, 224–240 (2015).
- Bailey, S. E. A morphometric analysis of maxillary molar crowns of Middle-Late Pleistocene hominins. *J. Hum. Evol.* **47**, 183–198 (2004).
- Xing, S. et al. Middle Pleistocene hominin teeth from Longtan Cave, Hexian, China. *PLoS ONE* **9**, 3114265 (2014).
- Kaifu, Y. Advanced dental reduction in Javanese *Homo erectus*. *Anthropol. Sci.* **114**, 35–43 (2006).
- Kaifu, Y. et al. Taxonomic affinities and evolutionary history of the early Pleistocene hominids of Java: dentognathic evidence. *Am. J. Phys. Anthropol.* **128**, 709–726 (2005).
- Gómez-Robles, A. et al. Geometric morphometric analysis of the crown morphology of the lower first premolar of hominins, with special attention to Pleistocene *Homo*. *J. Hum. Evol.* **55**, 627–638 (2008).
- Bailey, S. E. *Neanderthal Dental Morphology: Implications for Modern Human Origins*. PhD thesis, Arizona State Univ. (2002).
- Martín-Torres, M., Bermúdez de Castro, J. M., Gómez-Robles, A., Prado-Simón, L. & Arsuaga, J. L. Morphological description and comparison of the dental remains from Atapuerca-Sima de los Huesos site (Spain). *J. Hum. Evol.* **62**, 7–58 (2012).
- Martín-Torres, M. et al. Dental evidence on the hominin dispersals during the Pleistocene. *Proc. Natl Acad. Sci. USA* **104**, 13279–13282 (2007).
- Shang, H. & Trinkaus, E. *The Early Modern Human from Tianyuan Cave, China* (Texas A&M Univ. Press, 2010).
- Bowler, J. M. et al. New ages for human occupation and climatic change at Lake Mungo, Australia. *Nature* **421**, 837–840 (2003).
- Mellars, P. Why did modern human populations disperse from Africa ca. 60,000 years ago? A new model. *Proc. Natl Acad. Sci. USA* **103**, 9381–9386 (2006).
- Oppenheimer, S. The great arc of dispersal of modern humans: Africa to Australia. *Quat. Int.* **202**, 2–13 (2009).
- Armitage, S. J. et al. The Southern Route "Out of Africa": evidence for an early expansion of modern humans into Arabia. *Science* **331**, 453–456 (2011).
- Reyes-Centeno, H. et al. Genomic and cranial phenotype data support multiple modern human dispersals from Africa and a southern route into Asia. *Proc. Natl Acad. Sci. USA* **111**, 7248–7253 (2014).
- Westaway, K. E. et al. Age and biostratigraphic significance of the Punung Rainforest Fauna, East Java, Indonesia, and implications for *Pongo* and *Homo*. *J. Hum. Evol.* **53**, 709–717 (2007).
- Liu, W. et al. Human remains from Zhirendong, South China, and modern human emergence in East Asia. *Proc. Natl Acad. Sci. USA* **107**, 19201–19206 (2010).
- Reich, D. et al. Genetic history of an archaic hominin group from Denisova Cave in Siberia. *Nature* **468**, 1053–1060 (2010).
- Liu, W. et al. Late Middle Pleistocene hominin teeth from Panxian Dadong, South China. *J. Hum. Evol.* **64**, 337–355 (2013).

**Supplementary Information** is available in the online version of the paper.

**Acknowledgements** This work has been supported by the grants from the Chinese Academy of Sciences (KZD-EW-03, XDA05130101, GJHZ201314), National Natural Science Foundation of China (41272034, 41302016, 41271229), Netherlands Organisation for Scientific Research (NWO-ALW 823.01.003), Dirección General de Investigación of the Spanish Ministerio de Educación y Ciencia (CGL2012-38434-C03-02, and Acción Integrada España Francia HF2007-0115), Consejería de Educación de Junta de Castilla y León (CEN074A12-2) and The Leakey Foundation (through the support of G. Getty and D. Crook). We are grateful to several people who have provided access to comparative materials and/or advice in several aspects of the manuscript: R. Blasco, J. Rosell, J. M. Parés, M. Salesa, A. Tarrío, C. Saiz, I. Hershkovitz, A. Viallet, M. A. de Lumley, C. Bernis, J. Rascón and J. Svoboda. We are also grateful to Y.-S. Lou, L.-M. Zhang and P.-P. Wei who participated in the excavations at the Daoxian site.

**Author Contributions** X.-J.W., W.L. and M.M.-T. are the corresponding authors and have contributed equally to this work. X.-J.W. and W.L. are directing the Daoxian research project. W.L., M.M.-T., S.X., X.-J.W. and J.M.B.d.C. performed the anthropological study of the Daoxian human teeth. Y.-J.C. and S.-W.P. conducted the geological studies of the Daoxian site. Y.-J.C., R.L.E. and H.C. conducted the U–Th dating of the speleothem and stalagmite samples collected from the cave. M.J.S. conducted the palaeomagnetic analysis. X.-H.W. conducted the radiocarbon dating. H.-W.T. conducted the study of the faunal remains. X.-J.W., X.-X.Y., Y.-Y.L., W.L., Y.-J.C., H.-W.T. and S.-W.P. participated in the field research.

**Author Information** Reprints and permissions information is available at [www.nature.com/reprints](http://www.nature.com/reprints). The authors declare no competing financial interests. Readers are welcome to comment on the online version of the paper. Correspondence and requests for materials should be addressed to M.M.-T. (maria.martinon-torres@ucl.ac.uk), W.L. (liuwu@ivpp.ac.cn) or X.-J.W. (wuxiujie@ivpp.ac.cn)

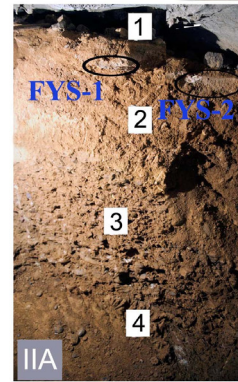
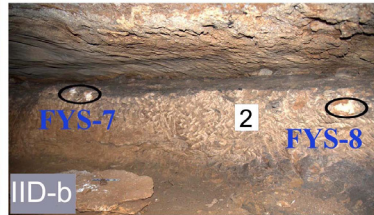
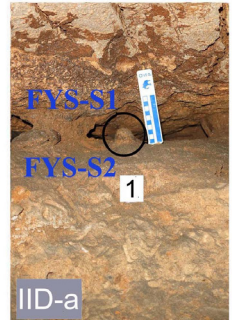
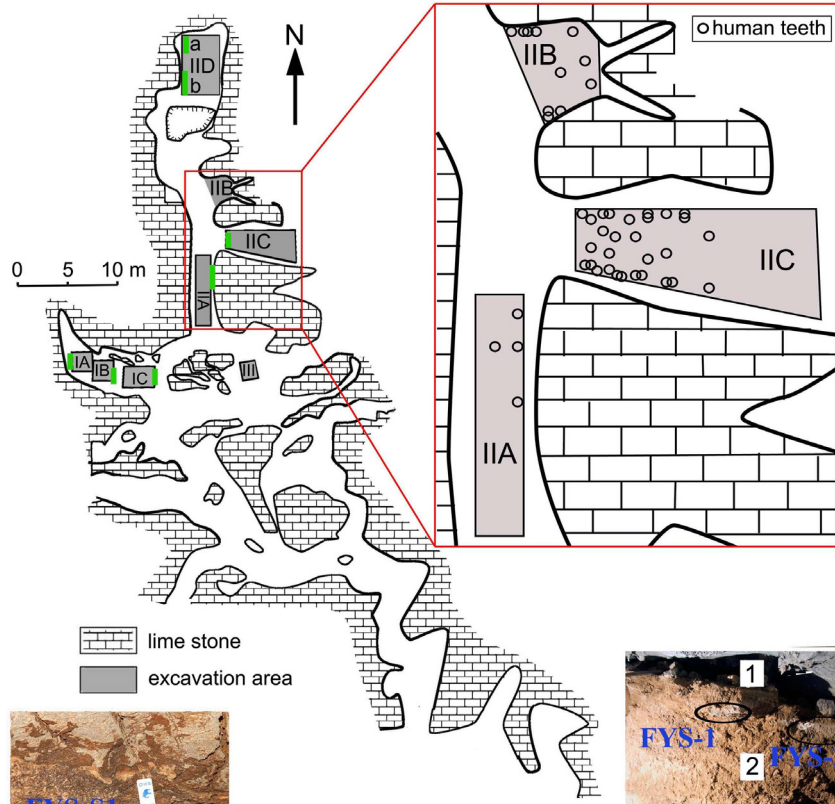
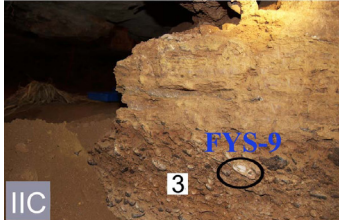
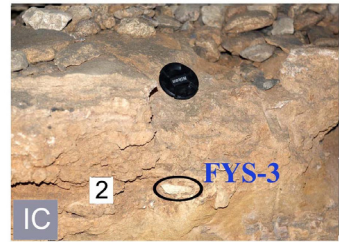
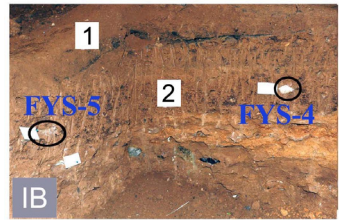
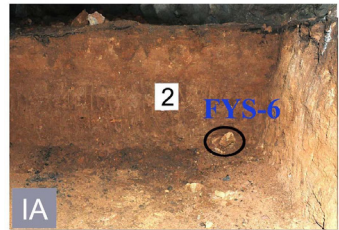
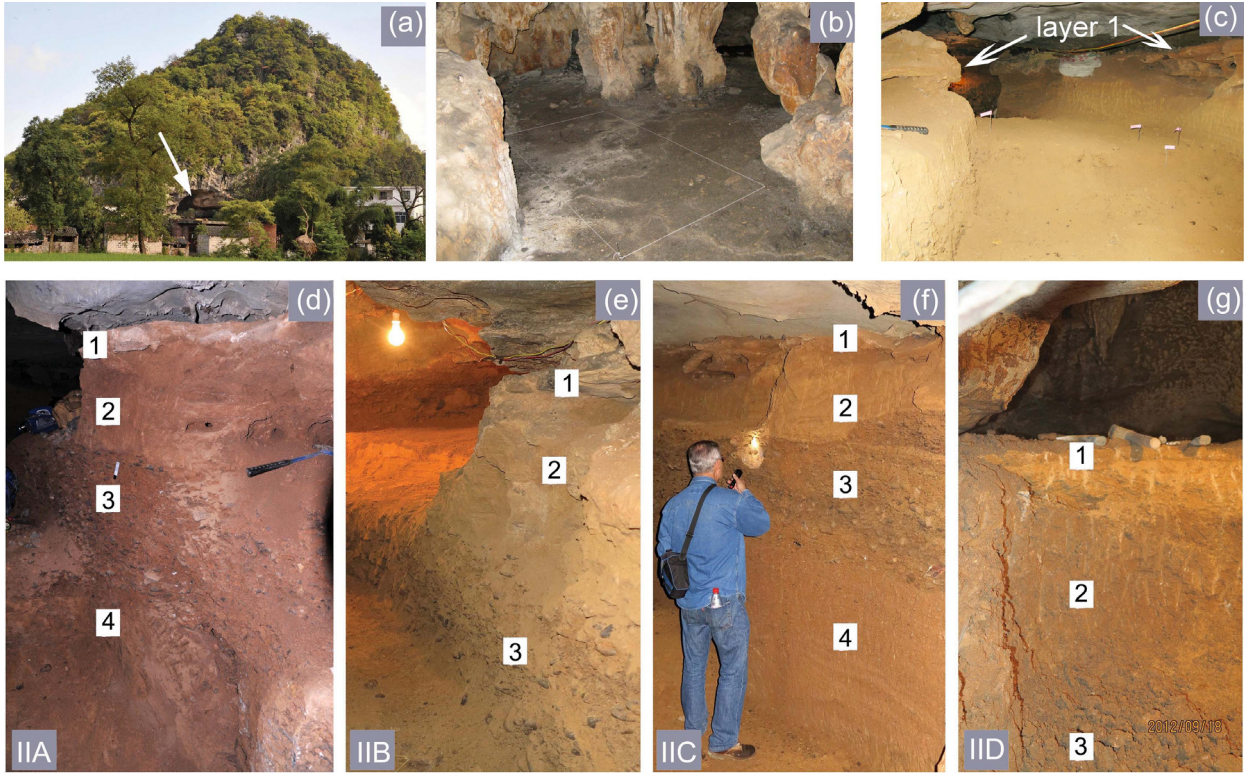
## METHODS

Description of the morphological features of the Daoxian hominin teeth follow the terminology usually used in dental studies<sup>17,29,30</sup>. To assess the morphological affinities of Daoxian teeth, we compared them to other Late Pleistocene samples from Africa, Asia and Europe (including Neanderthals), as well as a large contemporary *H. sapiens* sample (see Extended Data Table 3). Apart from both the descriptive comparative anatomy and the mesiodistal and buccolingual comparison, in the case of the M<sup>1</sup> we also calculated the relative cusp and occlusal polygon size.

For the metric comparison, the crown mesiodistal and buccolingual dimensions of the Daoxian teeth were measured with a standard sliding caliper and recorded to the nearest 0.1 mm. Bivariate plots of the mesiodistal and buccolingual diameters will be provided for the metric comparison of Daoxian with other hominin samples. To explore the Daoxian hominins in the context of the Middle to Late Pleistocene evolutionary changes in China, some Middle Pleistocene hominins from China were also included.

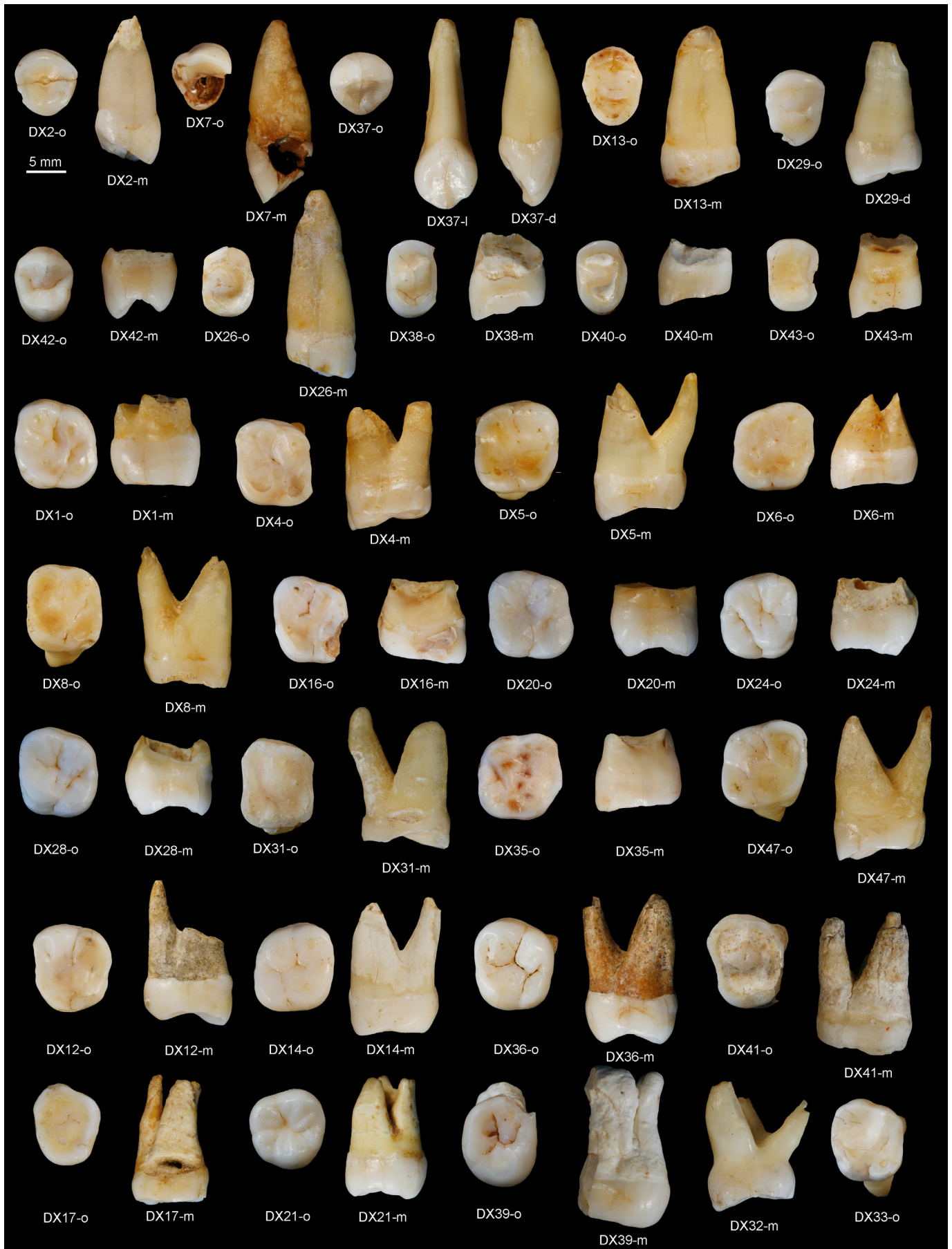
In addition, the total crown area and relative cusp area, and relative polygon areas for upper first molars were also measured and compared to a modern Chinese population. These features are considered to be taxonomically discriminative, particularly between *H. sapiens* and *H. neanderthalensis*<sup>11</sup>. The protocols for the measurement and calculation of the relative cusp areas of M<sup>1</sup> can be found in ref. 11.

29. Scott, G. R. & Turner, C. G. *The Anthropology of Modern Human Teeth: Dental Morphology and its Variation in Recent Human Populations* (Cambridge Univ. Press, 1997).
30. Weidenreich, F. *The Dentition of Sinanthropus Pekinensis: A Comparative Odontography of the Hominids* 1st edn (Geological Survey of China, 1937).
31. Li, Y. *et al.* A preliminary report on the 2011 excavation at Houbeishan Fuyan Cave, Daoxian, Hunan Province. *Acta Anthropol. Sinica* **32**, 133–143 (2013).
32. Wu, X. Z. *Yunxi Man: Excavation Report of the Huanglong Cave* (Science Press, 2006).
33. Jin, C. Z. *et al.* The *Homo sapiens* cave hominin site of Mulan Mountain, Jiangzhou District, Chongzhou, Guanxi with emphasis on its age. *Chin. Sci. Bull.* **54**, 3848–3856 (2009).
34. Yi, G. Liujian Man. *Fossils* **2**, 15 (1982).
35. Woo, J. Human fossils found in Kiukiang, Kwangsi, China. *Paleovertebrata Paleoanthropologica* **1**, 97–104 (1959).
36. Molnar, S. Human tooth wear, tooth function and cultural variability. *Am. J. Phys. Anthropol.* **34**, 175–189 (1971).
37. White, T. D. *et al.* Pleistocene *Homo sapiens* from Middle Awash, Ethiopia. *Nature* **423**, 742–747 (2003).
38. Rightmire, G. P. & Deacon, H. J. New human teeth from Middle Stone Age deposits at Klasies River, South Africa. *J. Hum. Evol.* **41**, 535–544 (2001).
39. Bräuer, G. & Mehlman, M. J. Hominid molars from a Middle Stone Age level at the Mumba Rock Shelter, Tanzania. *Am. J. Phys. Anthropol.* **75**, 69–76 (1988).
40. Chia, L. Note on the human and some other mammalian remains from Chgyang, Hupei. *Vertebr. Palasiat.* **1**, 247–257 (1957).
41. He, J. Preliminary study on the teeth of Jinniushan archaic *Homo sapiens*. *Acta Anthropol. Sinica* **19**, 216–224 (2000).
42. Wu, M. New discoveries of human fossils in Tongzi, Guizhou. *Acta Anthropol. Sinica* **3**, 195–201 (1984).
43. Wu, M., Wang, L., Zhang, Y. & Zhang, S. Fossil human teeth and associated cultural relics from Tongzi, Guizhou Province. *Vertebr. Palasiat.* **13**, 14–23 (1975).
44. Gu, Y. Zhoukoudian New Cave Man and their living environment. *Selected Papers in Paleoanthropology* 158–171 (Science Press, 1978).
45. Bae, C. J. *et al.* Modern human teeth from Late Pleistocene Luna Cave (Guangxi, China). *Quat. Int.* **354**, 169–183 (2014).
46. Chen, D. & Qi, G. Fossil human and associated mammalian fauna found from Xizhou, Yunnan. *Vertebr. Palasiat.* **16**, 33–46 (1978).
47. Dong, X. & Fan, X. Note on human fossil teeth from Fox Cave at Qingliu. *Acta Anthropol. Sinica* **15**, 315–319 (1996).
48. Huang, S. & Zheng, L. The upper Pleistocene human tooth and mammalian fossil from Changwu, Xhaanxi. *Acta Anthropol. Sinica* **1**, 14–17 (1982).
49. Li, Y., Wu, M., Peng, S. & Zhou, S. Human tooth fossils and some mammalian remains from Tubo, Liujiang, Guangxi. *Acta Anthropol. Sinica* **3**, 322–329 (1984).
50. Li, Y., Wu, M., Peng, S. & Zhou, S. Preliminary report on the investigation of Dingmo Cave in Tiandong County, Guangxi. *Acta Anthropol. Sinica* **4**, 127–131 (1985).
51. Peng, S. & Wang, W. Fossil of human beings and mammal discovered in Longdong Cave at Longlin, Guangxi. *Ethnoarchaeol. South China* **3**, 187–292 (1990).
52. Wang, W., Huang, Q. & Zhou, S. New found human tooth fossils in Tubo, Guangxi. *Longgupo Prehistory Culture* **1**, 104–108 (1999).
53. Wang, W. & Mo, J. Human fossil teeth newly discovered in Nanshan Cave of Fusui, Guangxi. *Acta Anthropol. Sinica* **23**, 130–136 (2004).
54. Wang, W., Huang, C., Xie, S. & Yan, C. Late Pleistocene hominin teeth from the Jimuyan Cave, Pingle County, Guangxi, South China. *Quat. Sci.* **31**, 699–704 (2011).
55. Wu, X. Z., Zhao, Z., Yuan, Z. & Shen, J. Report on paleoanthropological expedition of the Northeastern part of Kwangsi. *Vertebr. Palasiat.* **6**, 408–413 (1962).
56. Wu, X. & Zong, G. A human tooth and mammalian fossils of Late Pleistocene in Wuzhutai, Xintai, Shantong. *Vertebr. Palasiat.* **11**, 105–106 (1973).
57. Yu, J. Fossil man and cultural artifacts from Chuandong, Puding County, Guizhou Province. *J. Nanjing Univ. Nat. Sci.* **20**, 145–155 (1984).
58. You, Y., Dong, X., Chen, C. & Fan, X. A fossil human tooth from Qingliu, Fujian. *Acta Anthropol. Sinica* **8**, 197–202 (1989).
59. Zheng, L. A fossil human tooth from Zhaotong, Yunnan. *Acta Anthropol. Sinica* **4**, 105–108 (1985).
60. Zhou, G. & Yi, G. On the remains from Liuzhou region, Guangxi. *Mem. Beijing Nat. His. Mus.* **20**, 1–21 (1983).
61. Sládek, V., Trinkaus, E., Hillson, S. W. & Holiday, T. W. *The People of the Pavlovian: Skeletal Catalogue and Osteometrics of the Gravettian Fossil Hominids from Dolní Věstonice and Pavlov* (Dolní Věstonice Studies, 2000).
62. Bailey, S., Glantz, M., Weaver, T. D. & Viola, B. The affinity of the dental remains from Obi-Rakhmat Grotto, Uzbekistan. *J. Hum. Evol.* **55**, 238–248 (2008).
63. Quam, R., Bailey, S. E. & Wood, B. A. Evolution of M<sup>1</sup> crown size and cusp proportions in the genus *Homo*. *J. Anat.* **214**, 655–670 (2009).



**Extended Data Figure 1 | The Daoxian site.** **a**, Entrance to the Fuyan (Daoxian) Cave. **b**, Image of the intact flowstone in an unexcavated area. **c**, Detail of the excavation at region IIC. Pink flags point to *in situ* human findings. **d–g**, Detail of the stratigraphy of region IIA (**d**), IIB (**e**), IIC (**f**) and IID (**g**). In the centre, plan view of the excavation area at the Daoxian Cave. The

enlarged area shows the individual location of each human tooth. Lower pictures provide a detail of the location of each dating sample. FYS, speleothem fragment samples; FYS-S, stalagmite samples. For more details on the U-series results, see Table 1 and Supplementary Information E.

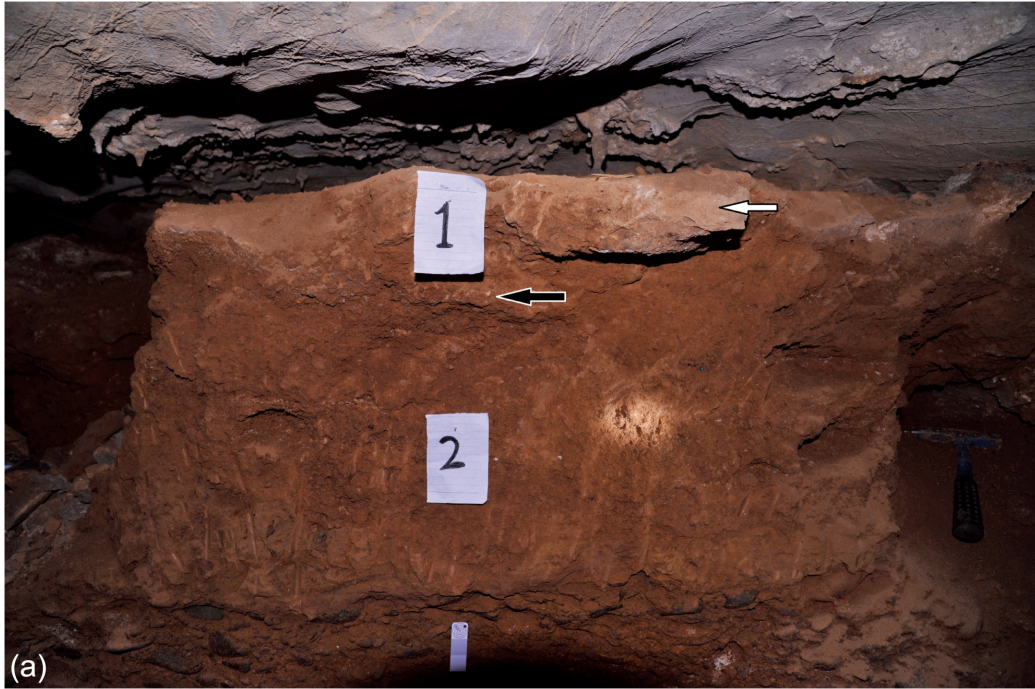


Extended Data Figure 2 | Daoxian upper teeth. Please see Extended Data Table 2 for detailed information. b, buccal; d, distal; l, lingual; m, mesial; o, occlusal.

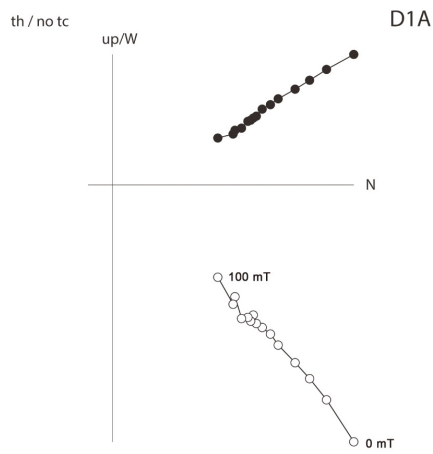




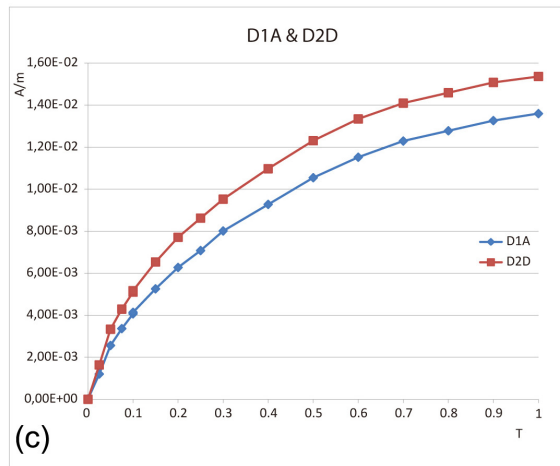
Extended Data Figure 3 | Daoxian lower teeth. Please see Extended Data Table 2 for detailed information.



(a)



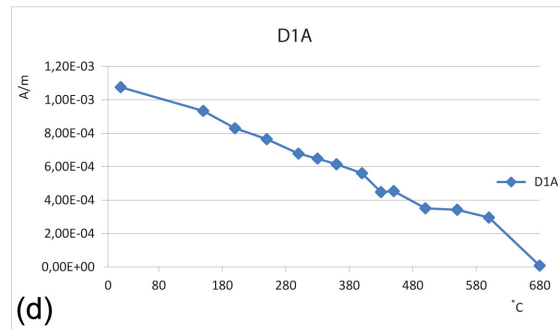
(b)



(c)



(e)



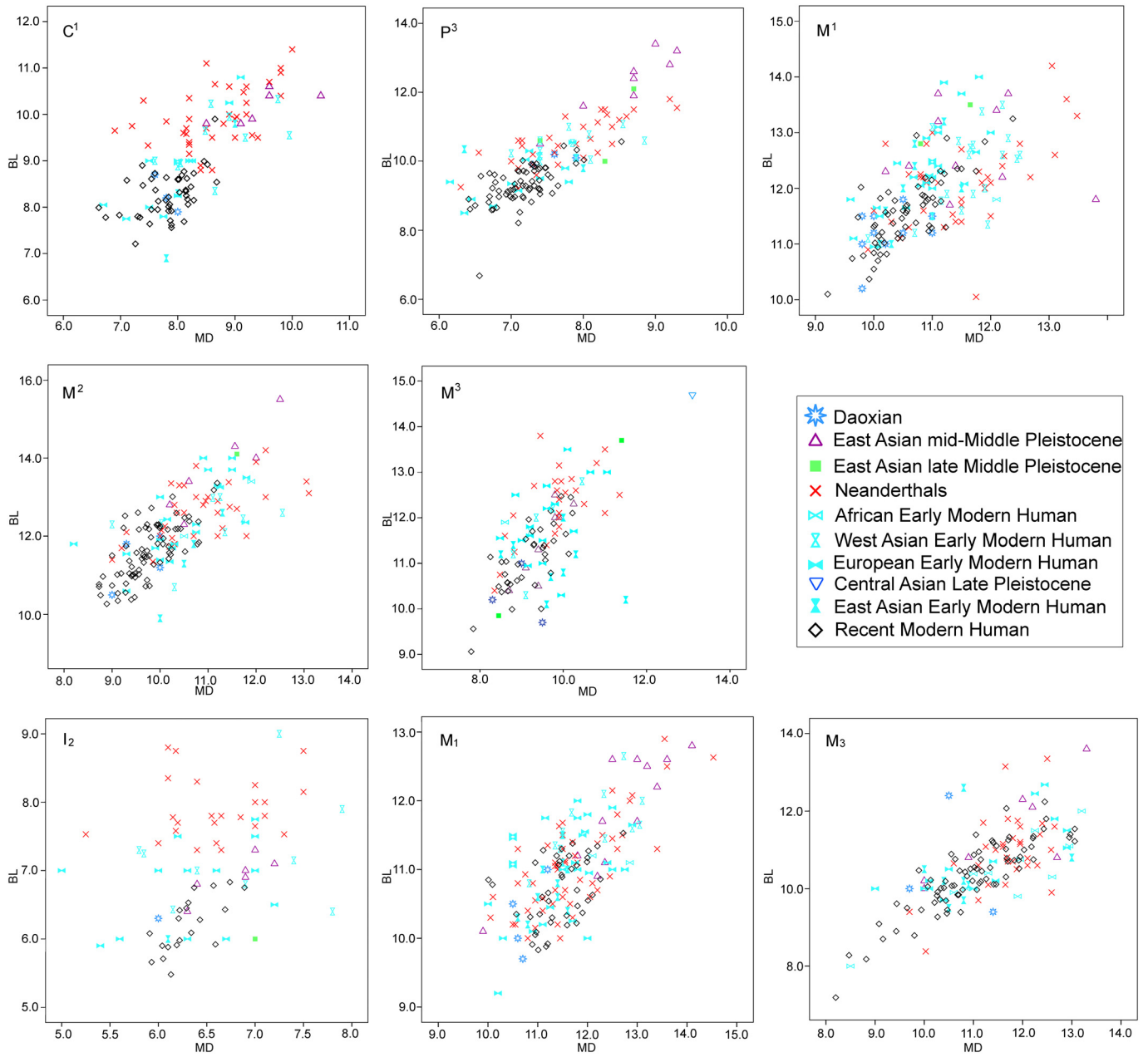
(d)

ID#	Demag type	DEC	INC	MAD	Q	AF/Tinf	AF/Tsup	NA/A	VGP λ	VGP Φ
D1A	AF	328	41	9.7	1	15 mT	100 mT	NA	57.6	356.2 E
D1D	Hybrid	311	37	10.7	2	15 mT	100 mT	A	43.8	9.1 E
D1E	TH	335	57	8.1	2	400 °C	590 °C	A	70.4	16 E
D2C	Hybrid	91	33	1.2	2	15 mT	70 mT	A	11.2	186.8 E
D2D	AF	101	31	3.9	1	15 mT	100 mT	NA	3.3	181.3 E
D2E	TH	94	37	4.1	2	250 °C	590 °C	A	10.8	182.9 E

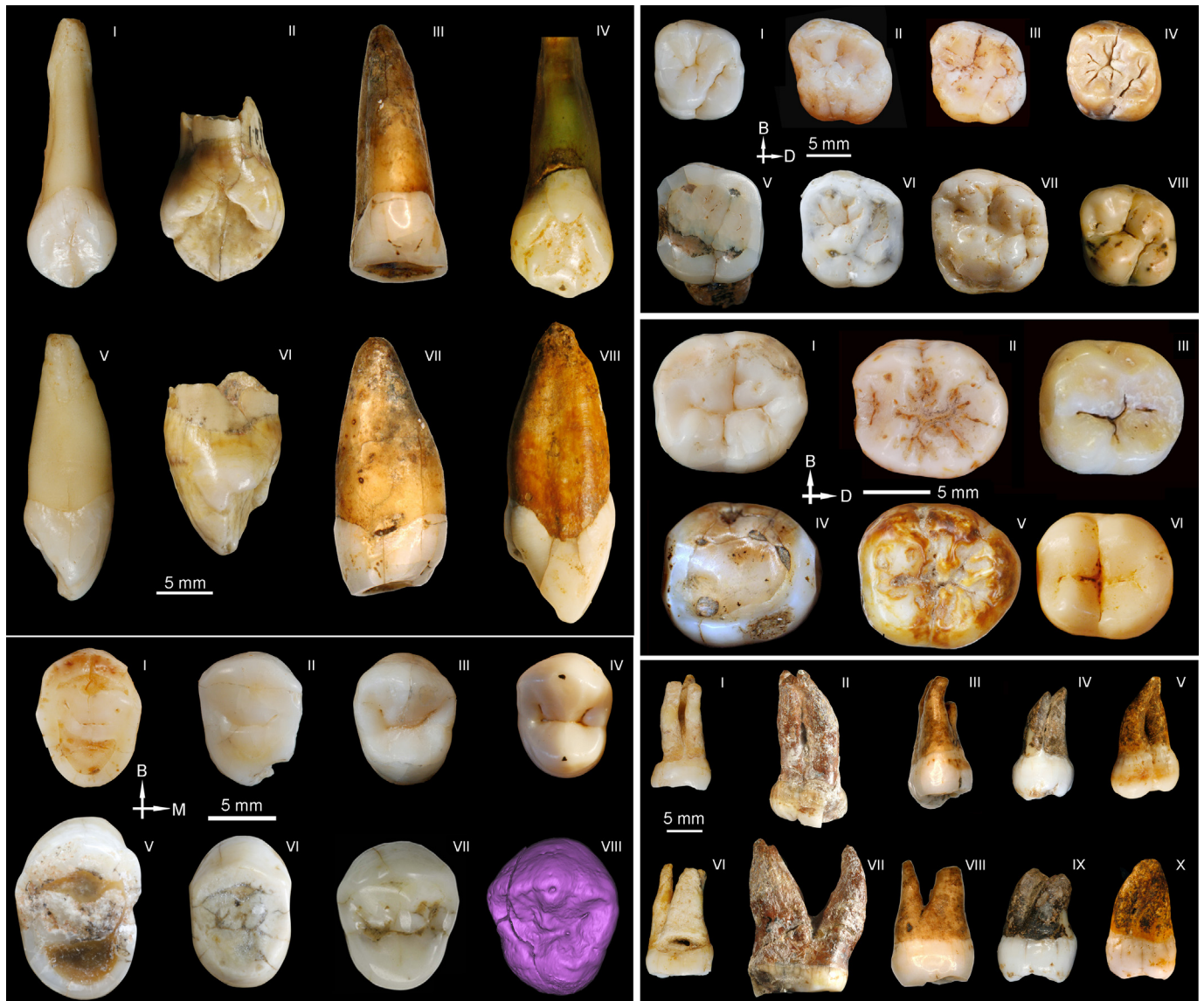
(f)

**Extended Data Figure 4 | Palaeomagnetic and rock-magnetic analysis of Daoxian flowstone.** **a**, Location of the orientated handsamples. White arrow indicates sample D1, black arrow indicates sample D2. **b**, Zijderveld diagram of alternating field demagnetized specimen D1A. Numbers next to the graph denote alternating field step in mT. **c**, Isothermal remanent magnetization (IRM) acquisition curve up to 1T for specimens D1A and D2D. **d**, Progressive stepwise thermal demagnetization of an IRM up to 1T of specimen D1A. **e**, Projection of virtual geomagnetic pole (VGP) of sample D1 with associated  $\alpha_{95}$ . **f**, Summary table of the thermal (TH), alternating field (AF), and hybrid

(both AF and TH) palaeomagnetic results. ID# denotes sample identification. A, anchored; DEC, declination of characteristic remanent magnetization (ChRM) direction; demag, demagnetization; INC, inclination of ChRM direction; MAD, maximum angular deviation; NA, not anchored; NRM, natural remanent magnetization; Q, quality index of ChRM direction, with 1 the highest quality and 2 the lowest; VGP, virtual geomagnetic pole latitude. AF/Tinf, lowest AF level or temperature step of ChRM in mT or °C; AF/Tsup, highest AF level or temperature step of ChRM in mT or °C.



**Extended Data Figure 5 | Metric comparison of Daoxian teeth.** Bivariate plots of the mesiodistal (MD) and buccolingual (BL) diameters of C<sup>1</sup>, P<sup>3</sup>, M<sup>1</sup>, M<sup>2</sup>, M<sup>3</sup>, I<sub>2</sub>, M<sub>1</sub> and M<sub>3</sub> of Daoxian and comparative samples.



### Extended Data Figure 6 | Morphological comparison of Daoxian teeth.

Comparative morphology of the Daoxian human teeth with other Pleistocene hominins and modern humans. Top left, upper canines. I, V: Daoxian (DX37); II, VI: Xujiayao (PA1480); III, VII: Huanglong Cave; IV, VIII: modern human. Bottom left: upper third premolars. I, II, III: Daoxian (DX13, DX 29, DX42); IV: modern human; V: Chaoxian; VI: Changyang (PA76); VII: Panxian Dadong (PA1577); VIII: Xujiayao (PA1480). Top right, upper first

molars. I: Daoxian (DX28); II: Neanderthal (Petit-Puymoyen Mx6); III: Qafzeh 5; IV: Tubo (PA1471); V: Hexian (PA836); VI: Chaoxian; VII: Xujiayao (PA1480); VIII: modern human. Middle right, lower second molars. I: Daoxian (DX30); II: Neanderthal (Hortus IV); III: Dolni Vestonice (DV37); IV: Huanglong Cave; V: Xintai; VI: modern human. Bottom right, upper third molars. I, IV: Daoxian (DX17), II, VII: Xujiayao; III, VIII: Huanglong Cave; IV, IX: Tubo (PA1476); V, X: modern humans.

Extended Data Table 1 | List of faunal composition at Daoxian and other Late Pleistocene localities of southern China

Fuyan Cave (Daoxian) <sup>31</sup>	Huanglong Cave <sup>32</sup>	Zhiren Cave <sup>33</sup>	Liujiang <sup>34,35</sup>
<i>Anourosorex squamipes</i>	+		
<i>Soriculus</i> sp.	<i>S. leucops</i>	+	
<i>Rhinolophus ferrumequinum</i>	+	<i>R. pearsoni</i>	
<i>Hipposideros armiger</i>	+	<i>H. pratti</i>	
<i>Eptesicus serotinus</i>			
<i>Murina leucogaster</i>	+		
<i>Tadarida insignis</i>			
<i>Trachypithecus</i> sp.	+	+	
<i>Macaca</i> sp.	<i>M. mulatta</i>	+	
<i>Hylobates</i> sp.	+	+	<i>Pongo</i> sp.
Pteromyidae indet.	<i>Belomys</i>	<i>Petaurista</i>	
<i>Rhizomys</i> sp.	+		
<i>Rattus norvegicus</i>		+	<i>R. rattus</i>
<i>Leopoldamys edwardsi</i>	+	+	
<i>Hystrix subcristata</i>	+	+	sp.
<i>Cuon javanicus</i>	+		sp.
<i>Ursus thibetanus</i>	+	+	sp.
<b><i>Ailuropoda baconi</i>*</b>	+		<i>A. melanoleucus</i>
<i>Martes flavigula</i>			
<i>Arctonyx collaris</i>	+	+	
<i>Lutra lutra</i>	+		
<i>Viverricula</i> sp.			
<i>Viverra</i> sp.	<i>V. zibetha</i>	+	
<b><i>Crocota ultima</i></b>	+		
<i>Panthera pardus</i>		+	+
<i>Panthera tigris</i>	+		sp.
<i>Prionailurus bengalensis</i>	+	<i>Felis</i> sp.	
<b><i>Stegodon orientalis</i></b>	+		+
<i>Elephas maximus</i>		+	
<b><i>Megatapirus augustus</i></b>	+	+	+
<i>Dicerorhinus sumatrensis</i>	<b><i>D. kirchbergensis</i></b>	<b><i>Rh. sinensis</i></b>	<b><i>Rh. sinensis</i></b>
<b><i>Sus</i> sp.</b>	<b><i>S. xiaozhu</i></b>	<b><i>S. cf. xiaozhu</i></b>	
<i>Sus scrofa</i>	+	+	sp.
<i>Moschus</i> sp.	<i>M. moschiferus</i>		
<i>Muntiacus muntjak</i>	+	sp.	sp.
<i>Cervus nippon</i>			sp.
<i>Cervus unicolor</i>	+	+	
<i>Capricornis sumatraensis</i>	+		
<i>Bos (Bibos) gaurus</i>	<i>Bubalus</i>		Bovidae indet.
Number of extinct large mammal species: 5	Number of extinct large mammal species: 9	Number of extinct large mammal species: 5	Number of extinct large mammal species: 3
Percentage of extinct species of large mammals: 19%	Percentage of extinct species of large mammals: 25%	Percentage of extinct species of large mammals: 25%	Percentage of extinct species of large mammals: 23%

Extinct species are marked in bold. References 31–35 are cited in the table.

Extended Data Table 2 | List and measurements of Daoxian teeth

Specimen Number		Tooth class	Side	Occlusal Wear degree	MD	BL	Date of discovery	Location and stratigraphic provenience
Field	Museum							
DX1	PA1543	M <sup>1</sup>	L	3	10.5	11.8	October 8, 2011	IIA Out of context
DX2	PA1544	C <sup>1</sup>	L	5	7.8	8.2	October 8, 2011	IIA Out of context
DX3	PA1545	P <sub>1</sub>	R	4	8.0	8.1	October 10, 2011	IIA Layer 2
DX4	PA1546	M <sup>1</sup>	L	4	(9.8)	10.2	October 10, 2011	IIA Layer 2
DX5	PA1547	M <sup>1</sup>	R	4	11.0	11.5	October 10, 2011	IIA Layer 2
DX6	PA1548	M <sup>1</sup>	R	4	10.2	11.0	October 11, 2011	IIA Out of context
DX7	PA1549	C <sup>1</sup>	R	5	7.6	8.7	October 13, 2011	IIA Layer 2
DX8	PA1550	M <sup>1</sup>	L	5	(10.0)	11.5	September 2, 2012	IIB Layer 2
DX9	PA1551	M <sub>2</sub>	L	6	11.0	10.5	September 3, 2012	IIB Layer 2
DX10	PA1552	M <sub>3</sub>	L	3	10.5	12.4	September 3, 2012	IIB Layer 2
DX11	PA1553	I <sub>2</sub>	L	4	6.0	6.3	September 3, 2012	IIB Layer 2
DX12	PA1554	M <sup>2</sup>	L	3	10.0	11.2	September 11, 2012	IIB Layer 2
DX13	PA1555	P <sup>3</sup>	L	4	7.6	10.2	September 11, 2012	IIB Layer 2
DX14	PA1556	M <sup>2</sup>	R	3	9.0	10.5	September 12, 2012	IIB Layer 2
DX15	PA1557	M <sub>1</sub>	L	4	11.2	11.0	September 19, 2012	IIB Layer 2
DX16	PA1558	M <sup>1</sup>	L	5	9.8	11.0	September 21, 2012	IIB Layer 2
DX17	PA1559	M <sup>3</sup>	L	6	8.3	10.2	September 22, 2012	IIB Layer 2
DX18	PA1560	C <sub>1</sub>	R	2	6.9	6.6	September 22, 2012	IIB Layer 2
DX19	PA1561	M <sub>2</sub>	L	6	10.5	10.3	September 23, 2012	IIC Layer 2
DX20	PA1562	M <sup>1</sup>	L	2	11.0	11.5	September 23, 2012	IIC Layer 2
DX21	PA1563	M <sup>3</sup>	R	0	9.5	9.7	September 23, 2012	IIC Layer 2
DX22	PA1564	M <sub>3</sub>	L	3	9.7	10.0	September 23, 2012	IIC Layer 2
DX23	PA1565	C <sub>1</sub>	L	2	6.8	7.4	September 23, 2012	IIC Layer 2
DX24	PA1566	M <sup>1</sup>	R	1	10.5	11.2	September 24, 2012	IIC Layer 2
DX25	PA1567	M <sub>1</sub>	R	6	10.7	9.7	September 24, 2012	IIC Layer 2
DX26	PA1568	P <sup>4</sup>	R	6	6.5	8.5	September 24, 2012	IIC Layer 2
DX27	PA1569	M <sub>3</sub>	R	3	11.4	9.4	September 24, 2012	IIC Layer 2
DX28	PA1570	M <sup>1</sup>	L	1	10.0	11.2	September 24, 2012	IIC Layer 2
DX29	PA1571	P <sup>3</sup>	L	3	7.9	10.1	September 24, 2012	IIC Layer 2
DX30	PA1581	M <sub>3</sub>	R	3	11.0	10.5	November 22, 2013	IIC Layer 2
DX31	PA1582	M <sup>1</sup>	L	6	(9.8)	11.5	November 22, 2013	IIC Layer 2
DX32	PA1583	dm <sup>2</sup>	R	5	9.8	10.4	November 22, 2013	IIC Layer 2
DX33	PA1584	dm <sup>2</sup>	L	4	8.6	10.2	November 22, 2013	IIC Layer 2
DX34	PA1585	P <sub>1</sub>	L	5	7.1	7.5	November 22, 2013	IIC Layer 2
DX35	PA1586	M <sup>1</sup>	R	5	11.0	11.2	November 22, 2013	IIC Layer 2
DX36	PA1587	M <sup>2</sup>	L	2	10.0	12.0	November 23, 2013	IIC Layer 2
DX37	PA1588	C <sup>1</sup>	R	2	8.0	7.9	November 23, 2013	IIC Layer 2
DX38	PA1589	P <sup>4</sup>	R	6	6.2	9.8	November 24, 2013	IIC Layer 2
DX39	PA1590	M <sup>3</sup>	R	2	9.0	11.0	November 24, 2013	IIC Layer 2
DX40	PA1591	P <sup>4</sup>	R	6	6.2	9.1	November 25, 2013	IIC Layer 2
DX41	PA1592	M <sup>2</sup>	L	6	9.3	11.8	November 26, 2013	IIC Layer 2
DX42	PA1593	P <sup>3</sup>	L	1	7.3	9.9	November 26, 2013	IIC Layer 2
DX43	PA1594	P <sup>4</sup>	R	6	-	9.0	November 26, 2013	IIC Layer 2
DX44	PA1595	M <sub>1</sub>	L	5	10.5	10.5	November 26, 2013	IIC Layer 2
DX45	PA1596	M <sub>1</sub>	R	5	10.6	10.0	November 26, 2013	IIC Layer 2
DX46	PA1597	M <sub>2</sub>	R	7	-	10.0	November 26, 2013	IIC Layer 2
DX47	PA1598	M <sup>1</sup>	R	5	11.0	11.5	November 27, 2013	IIC Layer 2

List of the Daoxian dental remains by tooth class with the degree of occlusal wear (following ref. 36) crown measurements, and region and stratigraphic position. L, left; R, right. Measurements are given in millimetres.

Extended Data Table 3 | Comparative material

Geography/ Chronology	Specimens	Sources of metrics
<b>Africa</b>		
Late Pleistocene	Herto, Klasies River Mouth*, Mumba	37-39
Holocene	Mesolithic North African sample* (Afalou, Tebessa, Aïn Meterchem, Gambetta, Aïn Dokkara, Taforalt)	
<b>East Asia</b>		
Mid-Middle Pleistocene	Chenjiawo*, Hexian*, Yiyuan*, Zhoukoudian ZKD)	12,30
Late-Middle Pleistocene	Changyang, Chaoxian*, Dingcun*, Jinniushan, Panxian Dadong*, Tongzi*, Xujiayao*, Zhoukoudian Locality 4	40-44
Late Pleistocene	Bailian Cave, Baojiyan, Changwu, Chuandong, Duan, Huanglong Cave*, Huli Cave, Jimuyan, Lipu, Liujiang*, Longlin Longdong, Longtanshan, Luna Cave, Nanshan Cave, Tiandong, Tianyuan Cave*, Tubo*, Xichou, Xintai*, Zhaotong, Zhiren Cave*, Upper Cave	45-60
Holocene and contemporary modern humans	Henan Province, Hubei Province	---
<b>Central Asia</b>		
Late Pleistocene	Denisova	27
<b>West Asia</b>		
Late Pleistocene	Qafzeh*, Skhul	Contributed by Wolpoff
Holocene and contemporary modern humans	Eynan*, Hayonim*, Nahal Oren*, Ohalo*	--
Neanderthals	Amud*, Tabun*, Kebara*, Shanidar	--
<b>Europe</b>		
Neanderthals	Arcy Grotte Renne*, Arcy Hyene*, Arcy Sur Cure (Mousterian), Chateaufort, Ehringsdorf, Genay (Côte d'Or), Gibraltar, Hortus, Krapina, Kulna, La Chaise, La Ferrassie, La Quina, Monsempron*, Le Moustier, Ochoz, Pech de l'aze, Petit Puymoyen, Regourdou, Saccopastore, Sakajia, Spy, St. Césaire, Subalyuk, Vindija	Contributed by Wolpoff
Late Pleistocene	Abri Pataud*, Brno, Combe Capelle, Dolní Věstonice*, Cro-Magnon, Fontchevade, Isturitz*, Le Rois*, Les Vachons, Mladeč, Pavlov, Predmostí, Saint Germain-La Riviere*, Zlaty Kun	Contributed by Wolpoff and <sup>61</sup>
Holocene and contemporary modern humans	Hispanic-muslim medieval collection of San Nicolás (Murcia, Spain)*, Mesolithic French sample* (Tévéc and Hoëdic), Neolithic French sample* (Avize, Dolmens de Bretons, Caverne de L'Homme Mort, Orrouy)	

Detailed list of the samples included in the morphological and metric comparison. Asterisk indicates that we examined the original fossil. For the rest, we used high resolution casts. References 37–61 are cited in the table.



**Extended Data Table 4 | Upper first molar relative cusp and occlusal polygon areas**

Samples	Protocone		Paracone		Metacone		Hypocone		Polygon	
	N	X±SD	N	X±SD	n	X±SD	n	X±SD	n	X±SD
Daoxian	6	32.5±1.0	6	25.9±1.4	6	22.3±1.3	6	20.3±1.3	4	34.0±1.8
Modern humans	50	30.9±1.1	50	27.0±1.4	50	21.8±1.5	50	20.3±1.6	24	37.5±5.4
Neanderthal	21	29.9±2.4	21	25.8±2.1	21	20.6±1.8	21	23.7±2.1	17	26.7±1.8
Qafzeh	7	31.3±2.3	7	24.8±1.6	7	21.3±2.5	7	22.8±5	4	33.3±2.7
LP HSAP	15	31.8±1.5	15	25.7±2.3	15	22.4±1.7	15	20.1±3	5	32.7±1.9

Data for Qafzeh and Late Pleistocene *H. sapiens* are taken from refs 62 and 63. Late Pleistocene *H. sapiens* (LP HSAP) sample is composed by Dolni Vestonice, Fontchevade, Laugerie Basse, Les Rois, Madeleine, Mladec, Patud, St Germaine-la-Rivière and Vachons.